Extracellular Hydrogen Peroxide Measurements Using a Flow Injection System in Combination with Microdialysis Probes – Potential and Challenges

Maria Moßhammer, Verena Schrameyer, Peter Ø. Jensen, Klaus Koren, Michael Kühl

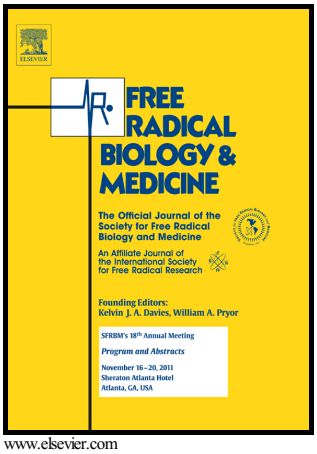

www.elsevier.com

PII: S0891-5849(18)30952-3
DOI: https://doi.org/10.1016/j.freeradbiomed.2018.05.089
Reference: FRB13791

To appear in: *Free Radical Biology and Medicine*

Received date: 10 January 2018
Revised date: 14 May 2018
Accepted date: 29 May 2018

Cite this article as: Maria Moßhammer, Verena Schrameyer, Peter Ø. Jensen, Klaus Koren and Michael Kühl, Extracellular Hydrogen Peroxide Measurements Using a Flow Injection System in Combination with Microdialysis Probes – Potential and Challenges, *Free Radical Biology and Medicine,* https://doi.org/10.1016/j.freeradbiomed.2018.05.089

Extracellular Hydrogen Peroxide Measurements Using a Flow Injection System in Combination with Microdialysis Probes – Potential and Challenges

Maria Moßhammer[1], Verena Schrameyer[1], Peter Ø. Jensen[2,3], Klaus Koren[1,4*] and Michael Kühl[1,5*]

[1] Marine Biological Section, Department of Biology, University of Copenhagen, Denmark
[2] Department of Clinical Microbiology, Rigshospitalet, Denmark
[3] Department of Immunology and Microbiology, Costerton Biofilm Center, Faculty of Health and Medical Sciences, University of Copenhagen, Denmark
[4] Department of Bioscience – Microbiology, University of Aarhus, Denmark
[5] Climate Change Cluster, University of Technology Sydney, Australia

[*] Correspondence: mkuhl@bio.ku.dk, klaus.koren@bios.au.dk

Abstract

There is a strong need for techniques that can quantify the important reactive oxygen species hydrogen peroxide (H_2O_2) in complex media and *in vivo*. We combined chemiluminescence-based H_2O_2 measurements on a commercially available flow injection analysis (FIA) system with sampling of the analyte using microdialysis probes (MDPs), typically used for measurements in tissue. This allows minimally invasive, quantitative measurements of extracellular H_2O_2 concentration and dynamics utilizing the chemiluminescent reaction of H_2O_2 with acridinium ester. By coupling MDPs to the FIA system, measurements are no longer limited to filtered, liquid samples with low viscosity, as sampling via a MDP is based on a dynamic exchange through a permeable membrane with a specific cut-off. This allows continuous monitoring of dynamic changes in H_2O_2 concentrations, alleviates potential pH effects on the measurements, and allows for flexible application in different media and systems. We give a detailed description of the novel experimental setup and its measuring characteristics along with examples of application in different media and organisms to highlight its broad applicability, but also to discuss current limitations and challenges. The combined FIA-MDP approach for H_2O_2 quantification was used in different biological systems ranging from marine biology, using the model organism *Exaiptasia pallida* (light stress induced H_2O_2 release up to ~2.7 µM), over biomedical applications quantifying enzyme dynamics (glucose oxidase in a glucose solution producing up to ~60 µM H_2O_2 and the subsequent addition of catalase to monitor the H_2O_2 degradation process) and the ability of bacteria to modify their direct environment by regulating H_2O_2 concentrations in their surrounding media. This was shown by the bacteria *Pseudomonas aeruginosa* degrading ~18 µM background H_2O_2 in LB-broth). We also discuss advantages and current limitations of the FIA-MDP system, including a discussion of potential cross-sensitivity and interfering chemical species.

Keywords:
Hydrogen peroxide, H_2O_2, ROS, Flow injection analysis, FIA, Microdialysis probe, Extracellular measurement, Optical sensor, Chemiluminescence

1. Introduction

Hydrogen peroxide (H_2O_2) is a reactive oxygen species (ROS) [1] and a strong oxidant, but relatively unreactive in comparison to other ROS [2]. The peroxide bond is nonetheless prone to cleaving due to heating, photolysis or

[*] *Abbreviations:* H_2O_2, hydrogen peroxide; ROS, reactive oxygen species; FIA, flow injection analysis; MDP, microdialysis probe; MDP-FIA, flow injection system coupled to a microdialysis probe; GOX, glucose oxidase; CL, chemiluminescent reagent; AE, acridinium ester; PMT, photomultiplier tube; ID, inner diameter; OD, outer diameter; LOD, limit of detection; LOQ, limit of quantification; DI, deionized water; LB medium, Luria-Bertani broth; PBS, saline phosphate buffer, F2 medium, enriched seawater medium; ASW, artificial seawater; FSW, filtered seawater

[*] Corresponding authors.
E-mail address: klaus.koren@bios.au.dk, mkuhl@bio.ku.dk

contact with redox metals [2,3]. These cleaving reactions can form the highly reactive hydroxyl radical ($HO^{\bullet}$). Its reactions have very low activation energy barrier and is one of the strongest known oxidants [2,4]; thus it is very important to understand the production and degradation processes of H_2O_2 as one of the main sources of $HO^{\bullet}$. Furthermore, H_2O_2 is of great importance in cell biology, where it plays a key role in important biochemical processes such as oxidative stress and as a transmitter of redox signals [2,5]. However, the exact role of H_2O_2 is often not fully understood due to uncertainties in the determination of real concentrations *in vivo* [6].

Some organisms such as algae [7] or human granulocytes (PMN) [8] release H_2O_2, while most cells and organism can sense and respond to H_2O_2 in their environment [5,9]. In many systems it is, however, still not possible to determine exact concentrations or monitor actual H_2O_2 dynamics, due to a lack of suitable techniques [6,9]. In an environmental context, H_2O_2 is released as an oxidative stress response by e.g. algae [10–15] or corals harboring microalgal symbionts [6,16]. H_2O_2 can also be formed via different (photo)chemical pathways in lakes [17,18], rivers [19,20], rainwater [17,19,21–25], geothermal springs [26] and open ocean seawater [19,27–30], and H_2O_2 has even been measured in thousands of years old ice cores [31,32]. In humans, H_2O_2 has been measured in exhaled air [33–35], urine [36,37], blood [38–40] or ocular fluids [41], and it functions as an important signaling agent between cells [42]. Hydrogen peroxide has also been linked to various diseases such as neurodegenerative diseases, Alzheimer's or lung infections [33,43,44] underlining the concentration-dependent dual character of H_2O_2 as a both harmful and important compound in biological systems. There is thus a strong need for methods that can quantify concentrations of H_2O_2 *in vivo* or under *in vivo*-like conditions with minimal sample manipulation. Such measurements are paramount for our understanding of the processes regulating the release and degradation of H_2O_2 in different environmental and biomedical systems.

Quantification of H_2O_2 is frequently attempted with optical techniques based on irreversible luminescent probes. Such approaches can be used to detect H_2O_2 via the luminescence intensity upon probe exposure giving valuable insights into hotspots and the presence of a species. However, correlating such changes in luminescence intensity to real H_2O_2 concentrations is difficult and often impossible [6]. A frequently used and well established technique for the determination of H_2O_2 in liquid samples is based on flow injection analysis (FIA) in combination with a H_2O_2-specific chemiluminescent reaction (Figure 1) [6,19]. This approach enables dynamic H_2O_2 concentration measurements in retrieved samples in near real time, where FIA overcomes the issue of the irreversibility of the underlying reaction scheme. Typically, such FIA-based systems consist of a valve system, which can switch between two modes (load and injection), a peristaltic pump ensuring a continuous flow of sample and reagents, and a photomultiplier tube coupled to a mixing cell for sensitive detection of the chemiluminescence intensity caused by the reaction of a chemiluminescent

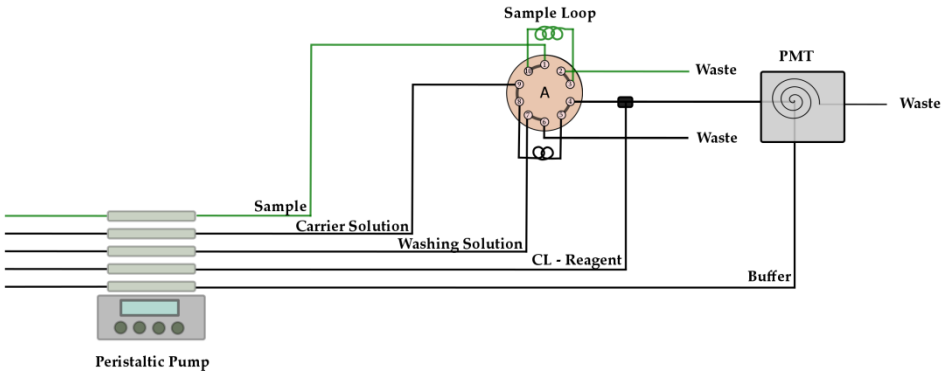

Figure 1: Schematic representation of a flow injection analysis (FIA) system used to quantify H_2O_2 in the load mode. The aggregate free sample is acquired with a sample tube and filled in the sample loop. When switching to injection mode, the sample is mixed with the chemiluminescent reagent (CL) and flushed by the carrier solution into a mixing chamber, where it is mixed with a buffer solution to adjust the pH and facilitate the reaction with the chemiluminescent reagent. The mixing chamber is optically coupled to a photomultiplier tube (PMT) detector that monitors the analyte-dependent chemiluminescence signal. Even flow of sample and reagents is facilitated with a peristaltic pump.

reagent (CL reagent) with the analyte of interest. Different chemistries such as luminol with a Co(II) catalyst [17,29,45–47] or the acridinium ester (10-methyl-9-(*p*-formylphenyl)-acridinium carboxylate trifluoromethanesulfonate) [19,48–51] have been used for H_2O_2 detection. Both chemiluminescence reaction schemes are pH dependent and show cross-sensitivities to Fe(II), which can however be overcome by working with buffered solutions and addition of FerroZine™ to complex freely available Fe(II) [45,48]. Temperature effects have to be taken into consideration as well, as chemiluminescent reactions are temperature dependent [52]. Luminol-based measurements are also influenced by other

analytes [45], while acridinium ester (AE) based measurements (employed in this study) are described as highly selective towards H_2O_2 in the literature [19,49]. However, we observed various media effects indicative of potential cross-sensitivity and interfering species, and we conducted a detailed study of cross-sensitivity and potential interfering species (see Supplementary information, results and discussion sections).

A major shortcoming of the overall FIA technique is its restriction to aggregate-free, liquid samples of low viscosity, as connectors and tubes are very narrow and block easily. Thus, the sample often needs a pretreatment step, such as filtering. Additionally, a relatively large sample volume (up to a few mL) is typically required, which can impose dramatic changes and artefacts in systems with a restricted volume and limits the spatio-temporal resolution. To overcome these limitations, we combined the FIA system with sampling via so-called microdialysis probes (MDPs) (Figure 2). Such probes are minimally invasive as analytes are retrieved from the sample via diffusion across a microdialysis membrane with a defined molecular cut-off into a perfusion solution. MDPs consist of a semipermeable membrane, which can be used to dialyze liquid, semisolid or solid media [53]; they were first developed for minimally invasive *in vivo* measurements of drug concentrations in tissue and organs of animals or humans [54]. MDPs can be applied *in vivo* as well as *in vitro*; they have been frequently coupled to different analytical systems, such as liquid chromatography, flow-through biosensors and capillary and microchip electrophoresis [55] and also allow measurements beyond liquid samples [53].

The analyte recovery by the MDPs is dependent on various factors, such as MDP membrane length, perfusion speed of the internal carrier solution or temperature, making it a tunable system for specific applications with a variety of sampling schemes [54]. In combination with a dynamic measurement technique such as the FIA system, MPDs can thus facilitate flexible measurements in a range of media and systems. In this study, we give a detailed presentation of a MDP-based FIA system for minimally invasive quantification of H_2O_2 concentration and dynamics. We give a detailed description of the novel experimental setup and its measuring characteristics along with different medical and biological applications to highlight its broad applicability, but also to discuss current limitations and challenges.

2. Materials and Methods

2.1. Chemicals and Stock Solution Preparation

10-Methyl-9-(phenoxycarbonyl)acridinium fluorosulfonate (catalog number: 68617) (AE), hydrogen peroxide (H_2O_2) solution, 30 % (w/w) (catalog number: 216763), catalase from bovine liver (catalog number: 1001937057), glucose oxidase from *Aspergillus niger* (catalog number: G7141-10KU), and FerroZine™ (catalog number: 160601) were purchased from Sigma Aldrich (sigmaaldrich.com). Na_2CO_3 was purchased from Riedel-deHaën (riedeldehaen.com; catalog number: 31432), HCl (37%) was purchased from Merck (merck-chemicals.com, catalog number: 1.01834.2500). The *Pseudomonas aeruginosa* strain used in this work was a catalase A negative PAO1 strain (Δ*katA*) [56]. Luria-Bertani (LB) broth was prepared from 5 g L^{-1} yeast extract (oxoid.com; catalog number: LP0021), 10 g L^{-1} tryptone-broth purchased from Oxoid (oxoid.com; catalog number: LP0042), and 10 g L^{-1} NaCl (merckmillipore.com; catalog number: 106404) at a pH of 7.5. F2 medium, i.e., an enriched seawater medium commonly used to culture marine microalgae, was prepared from filtered and autoclaved natural seawater supplemented with previously prepared stock solutions (final concentrations indicated in brackets): $NaNO_3$ (88.25 µM), $NaH_2PO_4 \cdot H_2O$ (31.26 µM), a trace metal stock solution containing ($FeCl_3$ (11.30 µM), Na_2EDTA (12.97 µM), $CuSO_4$ (0.040 µM), Na_2MoO_4 (0.025 µM), $ZnSO_4$ (0.077 µM), $CoCl_2$ (0.077 µM), $MnCl_2$ (1.430 µM)), as well as vitamin stock solution containing thiamine·HCl (vitamin B1; 296.5 nM), biotin (vitamin H; 2.047 nM), cyanocobalamin (vitamin B12; 0.3689 nM). All ingredients for these solutions were purchased from Sigma Aldrich). Artificial Seawater (ASW) was prepared from de-ionized water (DI water) and probiotic reef salt, purchased from Aquaforest (aquaforest.eu) and mixed according to the manufacturer's instructions, where the final ASW had a salinity of 35. The ASW was autoclaved before usage. MilliQ water, DI water and other carrier solutions were treated with 3 mg catalase L^{-1} for at least 30 minutes before further use, and were used to make all solutions. HCl as well as Na_2CO_3 and AE stock solution were added after the treatment of the DI water with catalase (3 mg L^{-1}, left for at least 30 minutes) to make a 0.01 M HCl solution, the 0.1 M Na_2CO_3 buffer solution (pH ~11.3) and the AE solutions. In experiments where free Fe(II) was expected, FerroZine™ was added to the AE solution to a final concentration of 250 nM. H_2O_2 stock solutions were freshly prepared every day, using untreated DI water. SI: NaCl, $CuCl_2 \cdot 2\ H_2O$, $FeCl_3 \cdot 6\ H_2O$, *tert*-butyl peroxide, urea, L-cysteine, glutathione, NaOCl and PBS were purchased from Sigma Aldrich (sigmaaldrich.com); ONOONa was purchased from BioNordika (bionordika.dk), NaOH as well as $MnSO_4 \cdot H_2O$ were purchased from Merck (merckmillipore.com), Agar was bought from PanReac AppliChem (applichemus.com) and $FeCl_2 \cdot 4\ H_2O$ from Fluka (fishersci.dk). The concentration of peroxynitrite (ONOONa) was determined via UV/VIS spectrophotometer (λ_{max} = 302 nM; $\varepsilon = 1670\ M^{-1}\ cm^{-1}$) according to the product information sheet.

2.2. Instrumentation

We used a flow injection analysis system (FeLume; Waterville Analytical) with the dedicated analysis software. The FIA system was coupled to a peristaltic pump (Dynamax, Rainin Instrument Company; shoprainin.com) and a syringe pump (Aladdin, World Precision Instruments; wpiinc.com) using PVC pump tubes (Tygon R3607, red/red) obtained from Glass Expansion (geicp.com). The tubing in-between valves in the FIA system consisted of fluoropolymer tubing (Upchurch Scientific® FEP; idex-hs.com). Microdialysis probes (CMA 7 Metal Free, 2 mm membrane length, with a cut-off of 6 kDa cut-off, cuprophane membrane (used for all measurements unless specified otherwise) and CMA 12 Metal Free, 4 mm membrane length, 20 kDa cut-off, polyarylethersulfone membrane polyarylethersulfone membrane (used for sub µM calibration, Figure S8 B)) were purchased from CMA (microdialysis.se, reference number: 8010772) and handled according to the manufacturer's guidelines, flushing it with ethanol prior to the first usage. Measurements of O_2 concentration were done with a FireStingGO_2 meter in combination with an OXR430 fiber-optic O_2 sensor or a respiration vial equipped with an O_2 sensor spot (OXVIAL20) that was monitored via the transparent glass wall of the vial with a bare fiber connected to the meter; all items were obtained from Pyroscience (pyro-science.com). Electrochemical measurements of H_2O_2 were done with a H_2O_2 microsensor (ISO-HPO-100) coupled to a free radical analysis system (both obtained from World Precision Instruments; wpiinc.com). Solutions were filtered through syringe filters (Whatman, 0.02 µm, 10 mm; Anatop^{TM} 10, gelifesciences.com; catalog number: 6809-1102). Samples were illuminated with a fiber-optic tungsten-halogen lamp equipped with a branched flexible light guide (KL1500, Schott.com), and incident light levels (400-700 nm) for different lamp settings were quantified in the samples with a submersible, spherical mini quantum sensor (US-SQS/L) coupled to a calibrated quantum irradiance meter (ULM-500) both purchased from Walz (walz.com).

2.3. Flow Injection Analysis (FIA) System Combined MDPs

The commercially available FIA system has a 10-port valve, which can be switched between load mode and injection mode (Figure 2) via the PC-controlled software. The system can be set up to also include a washing loop (e.g. diluted HCl) in order to clean the system tubings; this is e.g. relevant when using seawater in order to dissolve precipitates formed during the measurement [57]. The chemistry and chemiluminescent reaction for H_2O_2 measurements was described by King et al. [58]. Briefly, the chemiluminescent acridinium ester reagent (AE) reacts irreversibly with H_2O_2 forming an instable dioxetane complex, which releases energy in the form of light upon degradation to *N*-methylacridone under alkaline conditions. The chemiluminescence is detected by the PMT as a signal peak for a particular sample. In order to not over-saturate the PMT, signal intensities above ~1 million counts were avoided by adjusting the concentration of the chemiluminescent reagent. The peak integral can then be correlated – after prior calibration – to a specific H_2O_2 concentration. The MDPs allow the diffusive exchange of the analyte between the external sample medium and the inner, analyte-free probe perfusion medium, which are separated by a microdialysis membrane, with a specific molecular cut-off. A perfusion fluid (untreated DI water) is pumped through the dialysis probe at a certain speed, and is then transported into the 20 cm long sample loop of the flow injection system. The inner diameter (ID) of the FEP tubing used for the sample loop is 0.75 mm, which means the minimal sample volume is 88.4 µL (a small excess is however recommended to make sure the loop as well as the connectors are filled with bubble free sample solution). The sample loop is then flushed out by a catalase treated carrier solution, mixed with the AE reagent and transported into the reaction chamber in front of the PMT, where the pH is adjusted by a buffer solution (0.1 M Na_2CO_3, pH ~11.3). Switching back to 'sample mode' flushes the system with HCl (0.01 M) to keep the system from clogging due to precipitates (Figure 2.2).

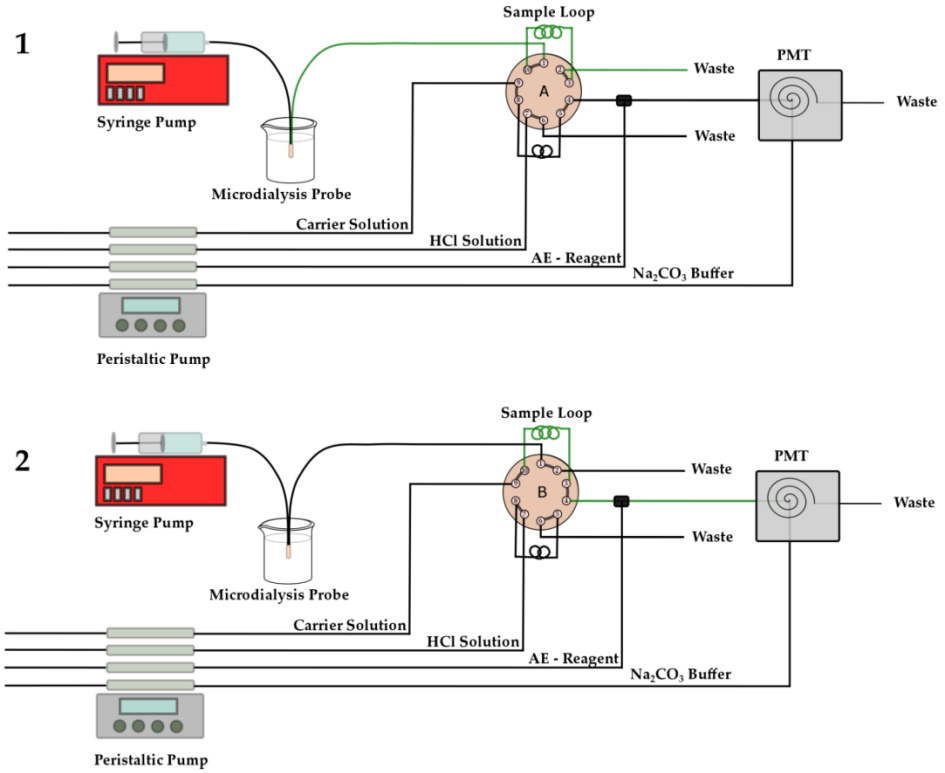

Figure 2: Load and injection mode of the FIA system coupled with the microdialysis probe (MDP). 1) Load mode. H_2O_2 is sampled via the microdialysis probe and guided into the sample loop. Excess solution will be flushed into the waste. Once the sample loop is filled, the 10-port valve can be switched to 2) injection mode. The sample solution containing H_2O_2 is flushed out of the sample loop, is mixed with the acridinium ester (AE) reagent and then transported into the detector mixing chamber by the carrier solution (such as catalase treated MilliQ water or seawater), where it is mixed with a buffer solution adjusting the pH. The microdialysis probe is operated by a syringe pump, where different speeds can be set. All other solutions (carrier solution, HCl solution / acid wash, chemiluminescent reagent (acridinium ester) and the Na_2CO_3 buffer are pumped through the system using a peristaltic pump.

2.4. Calibration With and Without MDPs

Calibration of the FIA system without the MDP connected (Figure 3A and Figure 4A) were done by adding defined volumes of the H_2O_2 stock solution (made in DI water) to the measurement medium. The same medium was used as carrier solution but treated with 3 mg L^{-1} catalase and filtered if necessary. For calibrations with the MDP connected to the FIA system (Figure 3A and Figure 4B), the perfusion-fluid pumped from the syringe through the MDP was untreated DI water, while DI water treated with 3 mg L^{-1} catalase was used as a reagent carrier solution and calibration solutions were stirred. As H_2O_2 has to enter the MDP via diffusion, a diffusion boundary layer establishes around the probe making it sensitive to stirring. The H_2O_2 stock solution was made in DI water and added to the stirred sample medium. For calibrations at elevated temperatures, vials containing the medium were heated to the required temperature, and H_2O_2 was only added right before measurement to avoid loss due to degradation. Real zero values were determined by adding catalase to a medium blank. The limit of detection (LOD) and limit of quantification (LOQ) were determined according to literature [59,60] by taking 3.3 times the standard deviation of the catalase treated blank divided by the slope of the calibration curve (LOD; equation 1) or 10 times the standard deviation of the catalase treated blank divided by the slope of the calibration curve (LOQ; equation 2).

$$\mathrm{LOQ} = \frac{3.3 * \sigma}{\mathrm{k}} \quad (1)$$

$$\mathrm{LOQ} = \frac{10 * \sigma}{\mathrm{k}} \quad (2)$$

Where σ is the standard deviation of the catalase treated blank (n = 3) and k is the slope of the calibration curve.

2.5. Calibration in Agar

1 wt% agar was dissolved in DI water using the microwave and 1 mL of the solution was pipetted in the plates to result in agar plates of 0.5 cm height. After cooling to room temperature, H_2O_2 stock solutions were pipetted on top of the agar plates and left to equilibrate for 3 h. H_2O_2 concentrations were measured within the agar plate and in the medium column above it.

2.6. Cross-Sensitivity Studies

Cross-sensitivity studies were mainly conducted with the direct inlet mode of the FIA system without MDPs. First, pH effects of the sample were tested (see Figure S2). A potential salinity effect was investigated by measuring H_2O_2 calibration curves with different NaCl backgrounds in DI water (0 g / 100 g, 5.1 g / 100 g, 15 g / 100 g and 21 g / 100 g DI water)(see Figure S3). Other potentially interfering species ($CuCl_2$, $FeCl_2$, $FeCl_3$, $MnSO_4$, *tert*-butyl peroxide, urea, L-cysteine, glutathione, NaOCl; ONOONa and $^1O_2$) were investigated by first measuring in a 50 µM H_2O_2 stock solution, and then in DI water treated with the potentially interfering species. Subsequently, the potentially interfering species was added to catalase treated MQ water to rule out the production of H_2O_2, which would interfere with the signal as well, and lastly the interfering species was measured with a 50 µM H_2O_2 background to rule out the reaction of the investigated species with H_2O_2 or quenching of the chemiluminescence (Figure S4-7).

2.7. Enzymatic Reaction Measurements

The experiment was conducted at room temperature in 200 mL of a stirred PBS buffered, glucose solution (1 mM), wherein H_2O_2 and O_2 were measured simultaneously (Figure 5) using a similar protocol of enzyme addition as in Koren et al. [61]. The sample solution was kept in a container sealed with a rubber stopper, to avoid O_2 leakage. The rubber stopper had three holes, one for the O_2 sensor, one for the MDP mounted on a glass rod, and one for the addition of the chemicals, which was sealed in-between reagent additions. Glucose oxidase (GOX) and catalase stock solutions were prepared in DI water (5 mg mL^{-1}). After baseline measurements, 0.125 mg GOX was added. The reaction was followed for 30 minutes. Then 0.125 mg catalase was added and the reaction was followed for 20 minutes. 0.250 mg GOX was added and the reaction monitored for 15 minutes. 0.500 mg catalase was added and the reaction followed for 15 minutes. Finally, 0.250 mg GOX was added together with additional 1mM glucose, and the reaction was followed until O_2 was consumed completely and no more H_2O_2 was produced. O_2 input via the MDP membrane was tested for in Figure S3.

2.8. H_2O_2 Dynamics in Light Stressed Sea Anemones

The sea anemone *Exaiptasia pallida* (strain H2) was transferred to a beaker containing aerated artificial seawater heated to 32°C. The organism was first kept in the dark for 60 minutes, while monitoring H_2O_2 (Figure 6) and O_2 levels. Subsequently, the sea anemone was exposed to high light (~1500 µmol photons m^{-2} s^{-1}; 400-700 nm) by irradiation from the side and top with a 2-branch flexible light guide connected to a fiber-optic tungsten-halogen lamp (KL1500, Schott). After ~80 minutes, the MDP was positioned in closer proximity to the animal than in the first position. The H_2O_2 build up due to light stress was followed for approximately 1 hour.

2.9. H_2O_2 Levels in LB Medium

The bacterium *Pseudomonas aeruginosa* was grown overnight at 37°C in an Erlenmeyer flask shaken at 170 rpm. Three falcon tubes were filled with 20 mL autoclaved and diluted LB medium (4mL LB + 16 mL DI) heated to 37°C and stirred within a heating block to ensure constant temperature. One tube was used to monitor H_2O_2 dynamics using the MDP - FIA system. The second tube was used to measure O_2 dynamics using a FireStingGO2. Every 10 minutes during the experiment, 1 mL samples were taken from this second tube, filtered via a 0.02 µm syringe filters (Whatman) into Eppendorf tubes and stored at 4°C over-night before measuring their H_2O_2 content via direct injection (FIA without a MDP) the following day. The third falcon tube was used to measure O_2 and H_2O_2 dynamics simultaneously using an electrochemical microsensor (ISO-HPO-100) coupled to a free radical analysis system (World Precision Instruments; wpiinc.com). Results are shown in the SI (Figure S2)). 2 mL of bacterial overnight culture were added to each of the stirred diluted LB media (37°C) resulting in a final density of approx. 2 x 10^8 CFU mL^{-1}. H_2O_2 and O_2 concentrations were monitored for 2 hours.

3. Results

We present the measuring characteristics of the combined MDP-based FIA measurement of H_2O_2, and illustrate various measurements optimization steps regarding reagent concentrations, syringe pump speeds and choice of sample

media. The design of the set-up allows minimally invasive sampling without removing sample volume, which enables a wide variety of application in environmental and biomedical science. We demonstrate the application of the combined MDP-FIA system for minimally invasive measurements of H_2O_2 dynamics in almost real time.

3.1. Calibration

In the commercially available FIA system, the aggregate-free sample is sampled via a tube and then guided through a FEP tube alongside the carrier, the buffer, the HCl wash and the AE solution. They are transported via the peristaltic pump with the same pump speed through the valve system – to avoid differences in pressure (e.g. buildup of

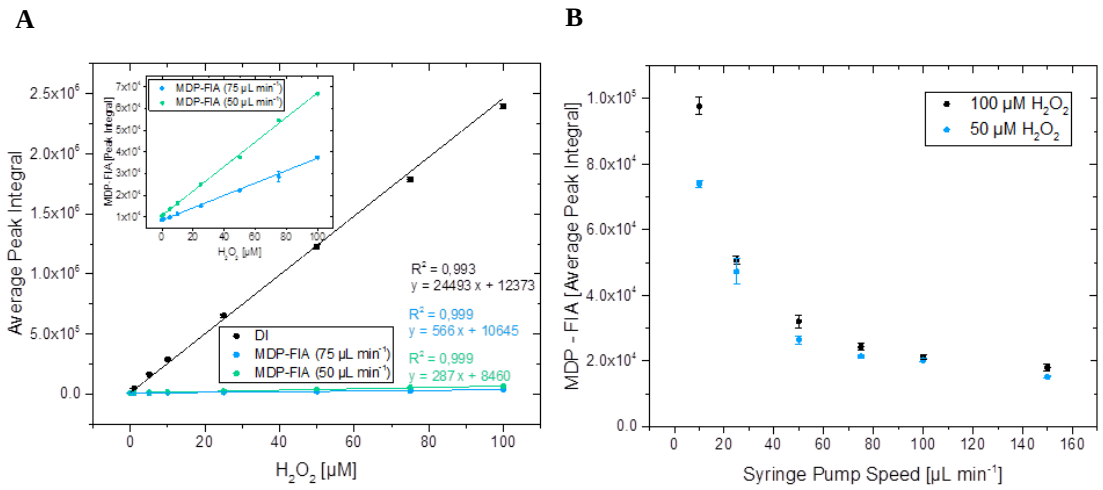

Figure 3: Comparison of H_2O_2 calibration curves measured with direct injection (DI) into the FIA system and via a microdialysis probe (MDP) coupled to the FIA system (MDP-FIA) using the same chemiluminescent reagent concentration. A) Shows the difference between calibrating with MDPs (blue and green) and without MDPs (black, n=3). The inset shows the effect of the syringe pump speed on the calibration curve using MDPs. The two shown pump speeds are 75 µL min^{-1} (blue; n=3) and 50 µL min^{-1} (green; n=1). B) Shows the decrease in in signal intensities between DI and MDP-FIA measurements, by plotting the ratio of the Peak Integral of the DI signal divided by the Peak Integral of the MDP-FIA signal at the respective pump speed for different H_2O_2 concentrations.

backpressure) within the system and to secure even flow speeds. A calibration curve of the 'direct injection' method (DI) is depicted in Figure 3A (black), using a 1 nM AE solution, a 0.1 M Na_2CO_3 buffer at pH 11.3, a 0.01 M HCl wash and MilliQ as carrier. All reagents were pre-treated with catalase according to literature [58] as described in the methods section. H_2O_2 standard solutions were prepared in untreated DI water and diluted in the measurement medium. In comparison, 2 calibration curves are depicted for the measurement with a MDP coupled to the FIA system (Figure 3A, blue and green). Sampling via a MDP connected to the FIA system (MDP-FIA) decreased the signal intensities, as the analyte recovery is diffusion limited and strongly dependent on external factors such as the syringe pump speed and MDP membrane characteristics (Figure 3A and B).

The measurement time was mainly influenced by the syringe pump speed, which is responsible for filling the 20 cm long sample loop, with a volume of ~88.4 µL (Table S1). The time needed for the sample solution to reach the sample loop also needs to be taken into consideration and this depends on the used tubes, their IDs and lengths. In our setup, the volume before the sample loop was ~50 µL. Thus the system response time - the time needed between sampling and signal out-put - comprises the time required to fill the sample loop plus the tubes connecting the MDP with the sample loop. However, once a continuous reaction is monitored only the time required for flushing the sample into the detector and refilling the sample loop needs to be taken into account in between measurements. The time necessary for flushing the sample out of the sample loop and through the detector can be monitored by observing the signal peak in the analysis software. The time depends on the pump speed of the peristaltic pump (here 1.8 mL min^{-1}), the length of tubing in between the sample loop and the detector as well as the geometry and volume of the flow cell. In our set-up the operational flushing time of the system was ~30 – 35 seconds.

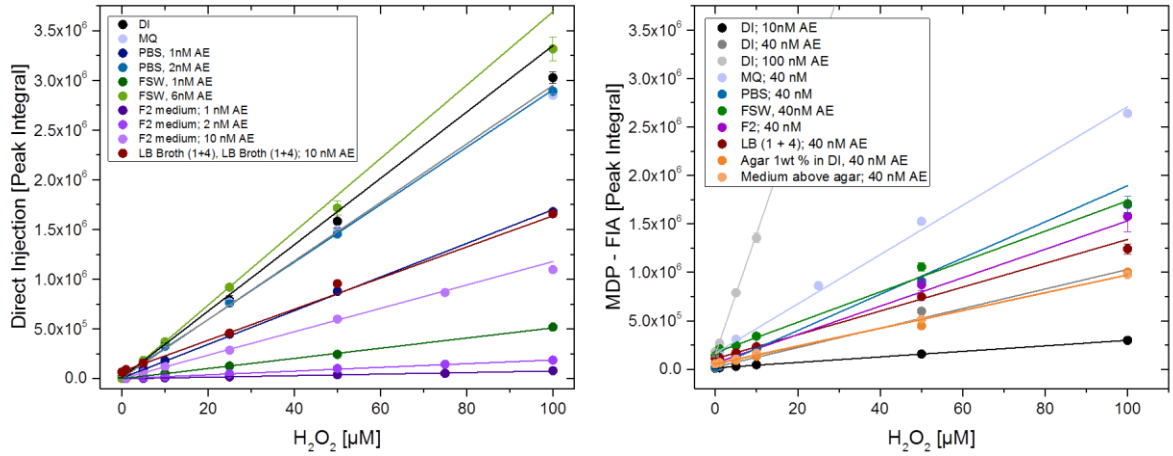

Figure 4: Effect of the chemiluminescent reagent (AE) concentration and the measurement medium composition on the H_2O_2 calibration curve. It is shown for DI water (black-grey), MilliQ water (light blue), PBS (blue), filtered seawater (FSW; green), F2 medium (purple), LB broth (red) and agar (1wt % in DI water; dark orange) as well as the liquid medium above the agar (orange) for the MDP-FIA system. A) Calibrations via direct injection (n=3). B) Calibrations using a MDP for sampling (n=3).

It is well known [54] that the analyte recovery with MDPs depends among other factors on the syringe pump speed. Figure 3B shows the difference in analyte recovery over different pump speeds for a 100 µM and a 50 µM H_2O_2 solution for the MDP-FIA system. However, the slope of the linear calibration curves cannot only be modified by changing the syringe pump speeds, but also by changing the concentration of the AE reagent or the measurement medium (Figure 4A and B). We performed calibrations in DI water, MilliQ water, filtered seawater (FSW), artificial seawater (ASW), F2 medium, PBS and LB broth as well as in agar (1wt% in DI water) and the overlaying medium using the MDP-FIA system. The AE reagent concentration was gradually increased until signal intensities in comparable ranges could be achieved, in order to compensate for medium effects and the reduced analyte recovery caused by the MDP. The DI water used for preparing the H_2O_2 stock solution was untreated to avoid degradation of the calibration solutions prior to measurement and each measurement was repeated 3 times (n=3). H_2O_2 background values were determined by measuring in untreated blank medium and catalase treated medium samples.

Measurements of H_2O_2 using direct injection into the FIA or using the combined MDP-FIA set-up exhibited highly reproducible and linear calibrations curves with small error bars for each particular setting of the various system parameters. If the system is switched off, it is however recommendable to recalibrate before measurement. Characteristics of the calibration curves in the different investigated media (shown in Figure 4) are given in Table 1 for the direct injection (DI) method as well as the MDP-FIA system, together with the used AE reagent concentrations aiming for an operational measuring range of 1 – 100 µM. The slope, R^2 value as well as the determined LOD and LOQ are given. LOD (Equation 1) and LOQ (Equation 2) were determined according to literature [59,60]. The slopes allow a comparison between the different calibrations and chosen chemiluminescent reagent (AE) concentrations. It can be used to estimate the AE reagent concentration necessary to get a calibration curve of a certain steepness, which however does not oversaturate the PMT at higher H_2O_2 concentrations. Here we aimed for a slope of ~ $1.2*10^4$ – $3*10^4$ counts · s per µM H_2O_2 for a calibration range between 1 – 100 µM.

Table 1: Overview of calibration curve characteristics in different media at room temperature using direct injection (DI) or MDP-FIA (the same membrane was used for all measurements) based measurements at a range of acridinium ester (AE) reagent concentrations enabling a measurement range of 1-100 µM H_2O_2. k denotes the slope of the calibration curve, while σ is the standard deviation of the baseline, i.e. the signal measured in the catalase treated blank.

Medium	**Injection Mode**	**AE reagent [nM]**	**Slope of the calibration curve** (k) [counts · s · (µM H_2O_2)$^{-1}$]	**R^2**	**LOD** (3.3*σ/k) [µM H_2O_2]	**LOQ** (10*σ/k) [µM H_2O_2]
DI water	DI	1	$3.34*10^4$	0.994	0.05	0.14
	MDP-FIA	10	$2.85*10^3$	0.999	0.56	1.7
		40	$1.01*10^4$	0.980	0.15	0.47
		100*	$1.24*10^5$	0.999	0.18	0.55
MilliQ water	DI	1	$2.95*10^4$	0.997	0.03	0.08
	MDP-FIA	40	$2.54*10^4$	0.996	0.16	0.49
PBS buffer	DI	1	$1.69*10^4$	0.999	0.03	0.09
		2	$2.89*10^4$	0.999	0.07	0.20
	MDP-FIA	40	$1.87*10^4$	0.990	0.60	1.8
Filtered Seawater (FSW)	DI	1	$5.11*10^3$	0.999	0.09	0.26
		6	$3.69*10^4$	0.999	0.01	0.02
	MDP-FIA	40	$1.57*10^4$	0.991	0.60	1.8
F2 medium	DI	1	$7.84*10^2$	0.994	0.13	0.40
		2	$1.87*10^3$	0.998	0.40	1.2
		10	$1.18*10^4$	0.997	0.05	0.14
	MDP-FIA	40	$1.47*10^4$	0.979	1.5	4.5
LB broth (1 + 4)	DI	10**	$3.03*10^4$	0.999	0.02	0.06
		10	$1.57*10^4$	0.998	0.05	0.14
	MDP-FIA	40	$1.23*10^4$	0.997	0.71	2.2
Agar	MDP-FIA	40	$9.20 * 10^3$	0.995	0.58	7.75
Medium Column above Agar	MDP-FIA	40	$9.15 * 10^3$	0.999	-***	-***

* Calibration between 0 – 50 µM H_2O_2; signal intensities too high for 100 µM due to PMT saturation.
** Calibration temperature was 37 °C and it was calibrated between 0 – 25 µM.
*** n=1; σ is not determined.

3.2. Cross-Sensitivity Studies

Different potentially interfering species on the AE-based H_2O_2 measurement were tested and the results are summarized in Table 2. Surprisingly, such tests are apparently lacking in the literature, albeit the AE method is promoted as being specific for H_2O_2 [48,57].

Table 2: Cross-sensitivities of potentially interfering chemical species on the AE-based H_2O_2 detection with the FIA system. Measurements were done in DI water, catalase treated MQ water as well as in combination with a 50 µM H_2O_2

background. Concentrations were chosen in regard to biological / physiological relevance as judged from the scientific literature. "-" indicates conditions that were not tested.

Investigated Species	Signal Change in DI water	Signal Change in Catalase Treated MQ water	Signal Change in Combination with 50 µM H_2O_2	Data
NaCl	Yes. Concentration dependent	-	Yes. Concentration dependent	Figure S3
Cu(II), 100 µM	No change	No change	No change	Figure S4
Fe(III), 200 µM	No change	No change	Increase	
Fe(II), 200 µM	Increase	Increase	Decrease	
Fe(II), 200 µM + FerroZine 250 nM	Increase	Increase	Decrease	
Mn(II), 10 µM	No change	No change	No change	
Ferrozine, 250 nM	-	-	Increase	
Tert-butyl peroxide, 50 µM	No change	No change	No change	Figure S5
Urea, 10 mM	No change	No change	No change	
L-cysteine, 100 µM	Decrease	Decrease	No signal	
Glutathione, 5 mM	Decrease	Decrease	No signal	
NaOCl, 50 µM	No change	No change	Increase ($^1O_2$ production)	Figure S6
ONOONa, 50 µM	Increase	-	-	Figure S7
ONOONa, 50 µM in PBS buffer	In PBS: Increase	In PBS: -	In PBS: -	

3.3. Applications

We tested the combined MDP-FIA system in a range of different samples in order to demonstrate its broad applicability and to discuss some of the current limitations of this new H_2O_2 measurement approach. The microdialysis probe was successfully applied to monitor the enzymatic reactions of glucose oxidase and catalase in a PBS buffered glucose solution (Figure 5). The MDP-FIA system was also applied for measurements of H_2O_2 production due to light-induced, photo-oxidative stress within an important model organism in symbiosis research; the sea anemone *Exaiptasia pallida* that harbors photosynthetic microalgae as symbionts in its tissue [62] (Figure 6). The MDP-FIA approach has the advantage here, that it allows the positioning in close proximity to the animal / in the bulk water close to the animal, without the danger of accidentally attaching the tube to the moving animal due to the suction of the tube or blocking the tube by aggregates in the water. Figure 6 shows the difference the positioning of the MDP in relation to the animal makes concerning a stable signal output; especially in a bubbled system. Finally, we looked at H_2O_2 dynamics in a bacterial culture (Figure 7). Calibration measurements in several media show high background levels of H_2O_2 in the blank; especially the commonly used bacterial culture medium LB showed elevated levels of H_2O_2 after autoclaving. Therefore, we investigated how bacteria (in this case Pseudomonas aeruginosa) deal with the external H_2O_2.

3.3.1. Enzyme reactions.

Glucose oxidase (GOX) was added to 200 mL stirred, PBS buffered glucose solution (1mM) at room temperature, resulting in a decrease in O_2 concentration approximately correlating with the stoichiometrically expected increase in H_2O_2 concentration (Figure 5). The observed decrease in O_2 concentration (taking a ~ 6 minute delay due to loading times in account) was ~63 µM O_2 while the H_2O_2 concentration increased by ~57 µM H_2O_2. When adding catalase, the H_2O_2 concentration decreased again, while the decrease in O_2 concentration was slowed down due to the O_2 produced by the reaction of catalase and H_2O_2. When reaching anoxia, the H_2O_2 production stopped and a decrease towards 0 µM could be observed due to continuous catalase activity.

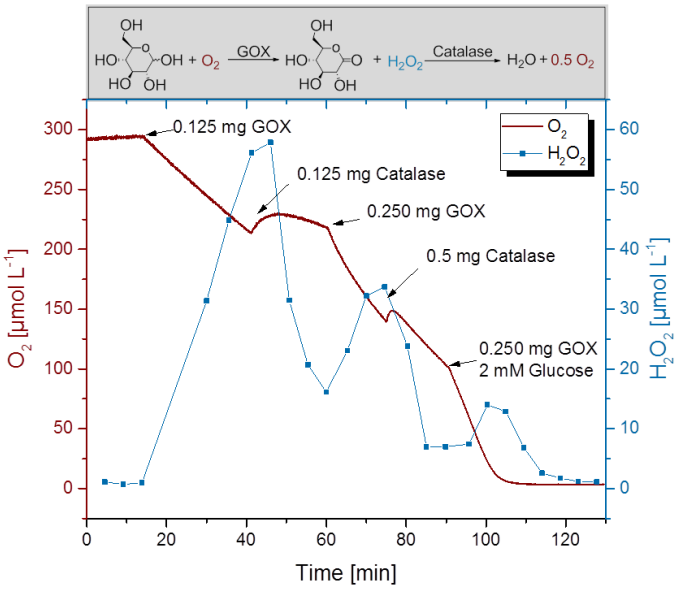

Figure 5: Monitoring of O_2 and H_2O_2 concentration dynamics in a PBS buffered 1 mM glucose solution upon alternating additions of glucose oxidase (GOX) and catalase. The enzymatic reaction schemes are shown above the data plot.

3.3.2. H_2O_2 dynamics in the sea anemone Exaiptasia pallida.

The sea anemone was kept for one hour in darkness (Figure 6; grey) where there was a visible decrease in the background H_2O_2 concentration from ~ 1.3 µM to 0.6 µM. When switching to high light, an immediate increase in H_2O_2 concentration was observed. In one approach the MDP was placed in proximity to the moving anemone (>1 cm distance). In a second approach, the MDP was in close proximity to the tissue of one of the sea anemone's tentacles (<0.5 cm). H_2O_2 increased up to similar apparent steady-state concentration in light of ~2.7 µM in both positions.

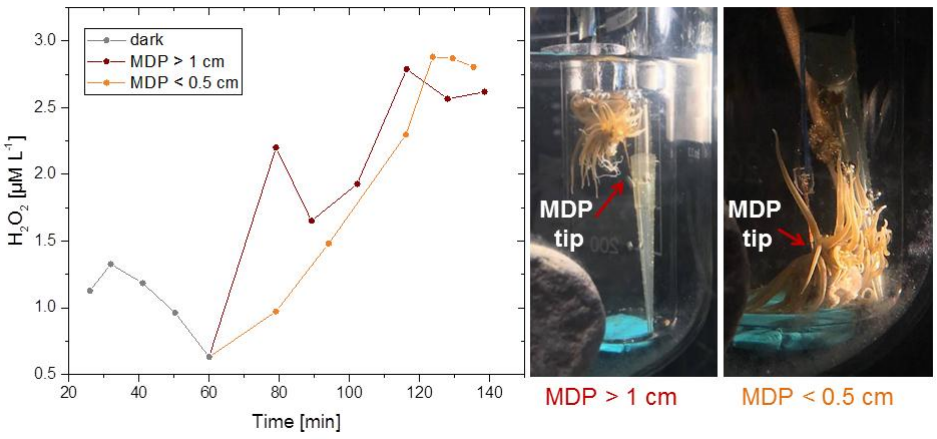

Figure 5: Monitoring of H_2O_2 dynamics at 32°C in the symbiont-bearing sea anemone *Exaiptasia pallida* in the dark (grey) and under light stress (~60 – 140 min) in two different measuring positions, with the MDP positioned >1 cm (orange) and <0.5 cm (yellow) from the tissue surface. The MDP was positioned in the bulk water surrounding the animal, but not in direct contact.

Measurements closer to the sea anemone tissue surface were less fluctuating.

3.3.3. H_2O_2 levels in LB medium.

A solution of the bacterium *Pseudomonas aeruginosa* was pipetted into stirred, heated (37°C) LB medium (indicated at ~10 minutes in Figure 7), which was monitored by an optical O_2 sensor, while H_2O_2 was measured either

via direct injection into the FIA or via a MDP inserted in the solution. Both H_2O_2 measurements via direct injection and via the MDP-FIA set-up showed a similar behavior, however, the direct injection measurement did not include blank values measured prior to bacteria addition. Therefore, the blank value of the calibration curve, which is LB medium without the addition of bacteria measured right before the experiment, is displayed to visualize the determined background concentration. The O_2 was depleted within 60 min, while the H_2O_2 concentration was depleted within 2-3 hours due to an apparent catalase activity in the bacterial solution. We note that the apparent blank value in the medium contained a significant amount of H_2O_2, which was then consumed by the bacteria.

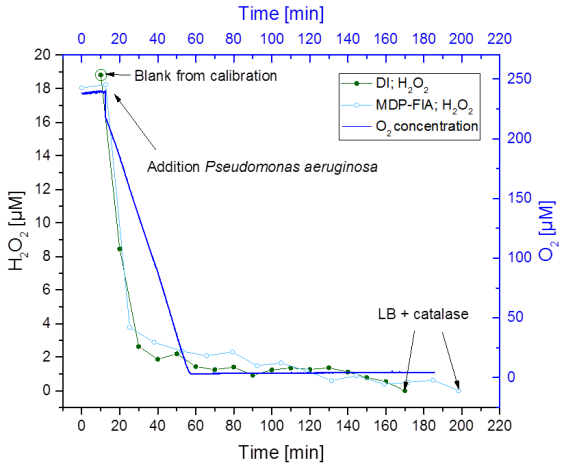

Figure 7: Monitoring of bacterial H_2O_2 and O_2 depletion in diluted, stirred LB growth medium at 37°C. The O_2 concentration (blue) was monitored by an optode, while H_2O_2 was measured with the combined MDP-FIA system (light blue) and with FIA system using direct sample injection (dark green). For the direct injection, the solution needed to be filtered (0.02 µm syringe filter) and was stored at 4°C in the fridge overnight before measurement. For the direct injection (dark green), no sample was taken and filtered for the blank before the addition of the bacteria, the blank from the calibration is depicted instead.

4. Discussion

We developed a flexible measuring setup for quantifying the important reactive oxygen species H_2O_2 by combining sampling via microdialysis probes (MDPs) with sensitive chemiluminescence-based detection of H_2O_2 on a flow injection analysis (FIA) system. In its current configuration, the combined MDP-FIA based systems enables quantification of H_2O_2 in a variety of aquatic samples and semisolid samples with high sensitivity (LODs and LOQs are shown in Table 1), linear calibration characteristics and a time resolution of ~4 min between measurements and ~6 minutes between samples. However, these system parameters can easily be modified e.g. by optimizing parameters such as the chemiluminescent reagent concentration, pumping speed of the system, tubing lengths and diameter, or choice of MDPs with different geometries and membrane characteristics. This system can now be used in a variety of environmental and biomedical samples.

As mentioned in the introduction, H_2O_2 can be found in natural waters. The formation of H_2O_2 in natural waters can be due to e.g. photochemical reactions of dissolved organic substances in the water [20]. However, background concentrations of H_2O_2 in other media, have to the best of our knowledge, not been studied in detail, especially when it comes to media used in the laboratory, such as DI water, MilliQ water, different seawater samples (ASW, FSW, F2 medium) or growth media used in microbiology such as LB-broth. To our knowledge, effects of water treatments such as autoclaving on the potential formation of background levels of H_2O_2 in liquid media have also not been studied. In order to determine such potential effects of media treatment and composition on H_2O_2 concentration a sensor system is required, which ideally allows continuous measurements in a broad variety of media. In liquid samples, the FIA system is well established as it allows continuous monitoring and can overcome pH interferences, which are often problematic for irreversible luminescent probes [6]. By combining the FIA system with a MDP we alleviated a major limitation of the FIA system, which is the need of pure samples. Small particulates such as cell or mineral aggregations or biofilms in the sample can block the narrow tubes of the FIA system, posing a need for sample cleaning or filtration steps. This extra treatment can be avoided by the MDP-FIA system, as the MDP functions as a filter to substances larger than the specific molecular cut-off of the microdialysis membrane. Thus no aggregates can get into the sampling tube, while H_2O_2 enters the perfusion solution in the MDP via diffusion across the microdialysis membrane. This can also reduce

the recovery of other potentially interfering species. In addition, it also allows measurements in semi-sold media, such as agar to measure directly in e.g. cell cultures.

The basic mechanisms described in literature to be responsible for H_2O_2 decay in natural waters are enzymatic removal (biological) and abiotic chemical reduction [28]. The O-O bond itself is relatively weak and prone to homolysis caused by heating, radiolysis, photolysis or the presence of redox metals, such as iron or copper [2]. Both of these redox metals are for example present in seawater and are even enriched in F2 medium. Higher temperatures are also frequently employed, especially in medical applications. This can lead to an accelerated degradation of the H_2O_2 calibration solutions over time and needs to be taken into consideration as well when calibrating and measuring in different media.

4.1. Calibration

As long as the PMT in the FIA system is not saturated, the system sensitivity can be tuned by modifying the chemiluminescent reagent (AE) concentration, pump speed and MDP membrane length enabling a broad calibration range (here tested for concentrations between 0 – 1000 nM (Figure S8: B), 0-10 µM (Figure S8: A) and 1-100 µM). Lower AE concentrations allow a broader operational working range (Figure 4), whereas the use of higher AE concentrations can be used to measure H_2O_2 in the nM to µM ranges (Table **1**). However, the increase in AE concentration increases the baseline as well. In theory, if the used solutions were completely H_2O_2 free, the baseline value should stay the same, but the FIA system is able to detect very low concentrations (in the pM range [19]) and thus the signal output can be influenced by residual amounts of H_2O_2. When catalase was added to the MilliQ or DI water (3 mg L^{-1}) used for the preparation of all solutions, the H_2O_2 background levels should be close to zero. This is however not true for the MDP perfusion-fluid which did not contain catalase to avoid degradation of the H_2O_2 diffusing into the perfusion fluid from the sample across the microdialysis membrane. It is also not true for the calibration standards, which contain the baseline H_2O_2 concentration of the specific medium. Such effects can be compensated for in the calibration procedure, by measuring in apparent zero H_2O_2 solutions before and after addition of catalase. This is necessary, as many real life systems can degrade H_2O_2 by releasing e.g. catalase, which then reacts with the background H_2O_2 as well as shown in our measurements in growth medium with bacteria (Figure 7). Therefore, it is important to know both the blank value and the real zero value in many applications when measuring H_2O_2.

4.1.1. Salt precipitation

Another issue, which needs to be considered is salt precipitation within the measuring system. At the working pH of ~11.3, seawater as well as F2 medium showed a white precipitate, most likely $Mg(OH)_2$ that is known to precipitate in seawater [49]. However, sodium carbonate can also form precipitates with other ions, e.g. Cu(II), Fe(II) or Fe(III). According to literature [1], the washing loop is sufficient to avoid excessive formation of the precipitate when working with seawater. However, as the combination with the MDP increased the loading time interval more precipitate formed, and the wash loop proved to be insufficient. Therefore, the pH buffer tube as well as the AE tube were flushed with HCl instead during the loading step. 2-4 minutes prior to switching to the inject mode, the system was flushed again with the buffer and the AE solution to allow the baseline value to stabilize. This also has the benefit of less consumption of the AE solution.

4.1.2. Syringe pump speed

Different syringe pump speeds were tested with a 2 mm long microdialysis probe membrane. However, the analyte recovery rate also depends on the MDP membrane length [54] and can thus be modulated by choosing MDPs with different dialysis membrane characteristics. With the MDPs having a 2 mm long membrane, pump speeds <50 µL min^{-1} gave sufficient measuring signals for H_2O_2 without introducing excessive loading times of the FIA sample loop (Table S1). For this experiment (Figure 3B), relatively high H_2O_2 concentrations were chosen (100 µM and 50 µM), but it is apparent that highest signal differences could be detected at the lowest syringe pump speed, thus resulting in a lower H_2O_2 detection limit. Overall, for our applications we chose a pump speed of 25 µL min^{-1}, which correlates to an initial ~6 minute cycle to fill all tubes (this however, strongly depends on the tube length and diameter). After initial sampling, the following measuring cycles only depend on the time required to fill the sample loop, which for our set-up involved a loading time of ~4 minutes (20 cm long tubes, ID: 0.75 mm). This means there is a slight delay in the system, but the values can be correlated to the specific sampling interval if all the tube lengths and IDs are known, or experimentally tested.

4.2. Medium effects and cross-sensitivity studies

We observed that the chemiluminescent signal and thus the apparent H_2O_2 level in different media can vary widely (Table 1, Figure 4). These effects were weak when comparing e.g. DI water to MQ water, while e.g. a strong

decrease in the detected signal was observed when switching from DI water to F2 medium or LB medium (Figure 4). These effects were strongest when using direct sample injection in the FIA system, where lower signals could e.g. be compensated for by increasing the AE reagent concentration. When using the combined MDP-FIA approach much less media effects on the chemiluminescent signal were observed and the same AE concentration could be used for all tested media in the MDP-FIA set-up. In the direct injection measuring mode, catalase treated medium was used as the carrier solution, which was directly mixed with the AE reagent and the buffer solution, and this resulted in more exposure to potentially interfering species. With the MDP-FIA set-up, the probe perfusion fluid is DI water (not the catalase treated medium), and the membrane of the MDP together with the chosen perfusion speed reduces the recovery of not only H_2O_2 but also of potentially interfering species. In addition, the external carrier in the MDP-FIA set-up is catalase treated DI water, which means that no raw sample medium is injected into the system. This also alleviates precipitation from seawater or potentially interfering ions, which are no longer directly injected into the system.

Depending on the sample medium, the observed changes in chemiluminescent intensity can have different reasons such as higher baseline concentrations of H_2O_2 in the medium, a strong change in pH or salinity, or a cross-sensitivity to another species. The effect of changing from DI water to other media is shown in Figure 4A (FIA) and Figure 4B (MDP-FIA) using identical settings and concentrations. Overall, some of the media effects can be attributed to precipitating salts from the artificial seawater and F2 medium, which affect the signal and can cause back pressure to build up in the system [49], or affect the scattering / absorption of the emitted photons in the AE reaction. F2 medium also has a high metal content. Cross-sensitivities of the AE reagent to other species (apart from Fe(II)) have not been reported in literature but were tested nonetheless to elucidate the underlying causes of these media effects. Changes in the sample pH only resulted in minor changes (Figure S2) and are usually buffered by the carbonate buffer. Changes in the salinity (NaCl concentration) influenced the slope of the H_2O_2 calibration curve relatively strongly (Figure S3). Salt concentrations should thus be kept stable and the experimental NaCl concentration has to be used for the calibration.

Regarding transition metals (Figure S4), Cu(II) and Mn(II) showed no interference with the system, neither in the presence nor in the absence of H_2O_2. Fe(III) showed no interference in the absence of H_2O_2, however, increased the signal in the presence of 50 µM H_2O_2 by almost 40%. Fe(II) interfered with the system in the absence of H_2O_2 as well as in the presence (50 – 60% of the signal peak integral of 50 µM H_2O_2).

The cross sensitivity to Fe(II) is compensated for in literature by the addition of FerroZine™ binding the Fe(II) before it can react with the AE solution[48]. Ideally, the FerroZine™ would be directly added to the MDP perfusion - fluid reservoir in the syringe pump. However, we wanted to avoid FerroZine™ diffusion out of the MDP membrane into the sample. The addition of FerroZine™ to the carbonate buffer solution would be too late, as by then the reaction with the AE reagent would have already taken place. Therefore, adding FerroZine™ to the AE solution was the best choice.

When trying to compensate for the Fe(II) cross-sensitivity by adding 250 nM FerroZine, an increase of approximately 120% in the signal peak integral for 50 µM H_2O_2 was observed in the absence of Fe(II). This increase might indicate that FerroZine™ acts as catalyst in the reaction of H_2O_2 with the AE, via an unknown mechanism. In the absence of H_2O_2 but the presence of 200 µM Fe(II), an increase in the DI water measurement (45% of the signal peak integral of 50 µM H_2O_2 in the presence of FerroZine™) and catalase treated MQ water (40% of the signal peak integral of 50 µM H_2O_2 in the presence of FerroZine™) was observed. 200 µM Fe(II) in the presence of 50 µM H_2O_2 and FerrZoine™ caused a drop in the apparent H_2O_2 signal peak integral down to 30% of the Fe(II)-free measurement. We conclude that FerroZine™ is not suitable to overcome the Fe(II) cross-sensitivity in the AE-based H_2O_2 detection in our setup. However, it might be used to enhance signal intensities for low H_2O_2 concentrations. Other complexing agents like e.g. EDTA may be suitable for removing the Fe(II) cross-sensitivity, but remain to be tested.

Different biomolecules such as urea, L-cysteine, glutathione and *tert*-butyl peroxide were also tested for their interference on the AE-based H_2O_2 detection (Figure S5). *Tert*-butyl peroxide as well as urea showed no significant interference, neither in the absence nor in the presence of H_2O_2. A minor decrease (~96%) of the signal peak integral for 50 µM H_2O_2 was observed in the presence of urea. However, a reaction of urea with H_2O_2 is more likely than the interference with the chemiluminescent reaction. L-cysteine and glutathione caused the chemiluminescent signal to drop below the baseline in the absence as well as the presence of H_2O_2. This drop indicates a degradation of H_2O_2 in the presence of these two antioxidants and a complete removal of the background H_2O_2 rather than a cross-sensitivity. High amounts of L-cysteine or glutathione can thus strongly affect measurements of H_2O_2 concentration.

Another investigated species was hypochlorous acid (Figure S6). In the absence of H_2O_2, no change in the system was detected (besides a slight increase in the measured baseline after adding 1 mM). However, in the presence of H_2O_2 an increase in the signal of ~126% was observed. As hypochlorous acid showed no reaction in the absence of H_2O_2, we conclude that the interfering species probably is singlet oxygen ($^1O_2$) resulting from the reaction of hypochlorous acid with H_2O_2 [63]. However, as $^1O_2$ is very short lived (µs range, dependent on temperature and solvent [64]) the observed interference could be alleviated by the introduction of the MDP in the sampling step (Figure S6) and might even be further reduced by a reduction of the MDP perfusion speed.

Peroxynitrite ($ONOO^-$) was investigated as well for its potential ability to interfere with the AE-based H_2O_2 measurement (Figure S7). $ONOO^-$ levels were chosen according to literature where it is described in µM concentrations (between ~55 µM in serum and 2.8 µM in saliva [65]). The $ONOO^-$ stock concentration was determined right before the experiment according to the product information by the provider using a spectrophotometer (λ_{max} = 302 nM; ε = 1670 M^{-1} cm^{-1}). The experiment showed strong cross-sensitivity to peroxynitrite, as the signal peak integral in DI water exceeded the 50 µM H_2O_2 peak integral by almost 92 % in the presence of peroxynitrite; even coupled to the MDP, where the increase in the peak integral was even higher. Peroxynitrite is supplied in a solution of 0.3 M NaOH, where it has according to the provider a half-life, at room temperature of 5 hours; whereas at pH 7.4 it is supposed to have a half-life of a few seconds [66]. Thus, the cross-sensitivity to peroxynitrite was investigated in PBS buffer at a pH of 7.4 as well. There was an even stronger cross-sensitivity visible when using PBS (the signal for 50 µM H_2O_2 concentration in PBS was exceeded by almost 300%). We speculate, whether the cross-sensitivity is caused by peroxynitrite or one of its degradation products. Peroxynitrite degrades at acidic conditions to $\bullet NO_2$ and $HO\bullet$, and regarding the observed interferences when measuring in the presence of Fe(II) and Fe(III) together with H_2O_2, the strong apparent interference might be caused by the hydroxyl radical instead of peroxynitrite. According to the manufacturer, ONOONa was produced via H_2O_2, so a certain background concentration of H_2O_2 cannot be ruled out.

In general, higher baselines can be an indication for H_2O_2 present in the blank (e.g. LB broth; Figure 7), which can be compensated for by the addition of catalase. If the baseline decreases below the initial blank value after addition of catalase, the difference can be assumed to be due to the background H_2O_2 concentration for the given medium/solution.

We conclude that irrespective of the various mechanisms causing such media effects, careful calibration and optimization for a given application can alleviate the effects and resulted in highly linear calibration curves for H_2O_2. However, there are various cross-sensitivities which need to be taken in consideration before starting an experiment. The system as described can be used for many applications, but due to the found cross-sensitivities there can be certain applications were it cannot be used as a reliable specific quantification of H_2O_2 alone, but rather for quantification of ROS or oxidative stress indicator.

4.3. Enzyme Reaction.

The MDP was used in combination with an optical O_2 sensor to follow the reaction dynamics of glucose oxidase (GOX) and catalase in a PBS buffered glucose solution (Figure 5). Upon addition of GOX, glucose and O_2 reacted producing H_2O_2, as quantified by the combined MDP-FIA system. Upon addition of catalase the formed H_2O_2 was degraded according to the reaction Scheme 1.

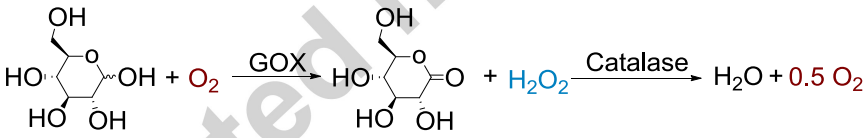

Scheme 1: Enzymatic reaction of GOX with glucose in the presence of O_2 producing H_2O_2, which is subsequently degraded into O_2 and water upon addition of catalase.

This resulted in a temporary increase in O_2 concentration. However, as more O_2 was degraded than produced O_2 depletion was observed. The addition of GOX as well as catalase was repeated to demonstrate the capability of the MDP-FIA system to monitor dynamic H_2O_2 concentration changes. In the first addition step, the decrease in O_2 was higher than the increase in H_2O_2 probably due to the time delay between the FIA system response (6 minute cycle time) and the immediate response of the O_2 sensor. When looking at the O_2 signal 6 minutes prior to the addition of catalase the overall decrease in O_2 concentration was 63 µM, while the corresponding increase in H_2O_2 concentration was 57 µM, which was approximately in accordance with the reaction scheme stoichiometry. The combined MDP-FIA system is thus well suited to monitor dynamic H_2O_2 changes in solutions due to enzymatic reactions or other (bio)chemical processes. Such measurements are highly relevant in both environmental and biomedical sciences.

4.4. H_2O_2 Dynamics in the Sea Anemone Exaiptasia pallida.

In a second application, we assessed the H_2O_2 production of the anemone *Exaiptasia pallida* (strain H2) under a global change relevant stress scenario [67], i.e., increased seawater temperature (32°C) and high irradiance (1500 µmol photons m^{-2} s^{-1}). *Exaiptaisa pallida* is commonly used in ecophysiological and biomolecular research as a model organism for cnidarian-coral symbioses [68], and technical advances in the assessment of quantitative H_2O_2 production of such organisms under oxidative stress are in strong demand. Besides the very first successful detection of light-stress induced H_2O_2 formation in *Exaiptasia*, we could also show that the positioning of the MDP has a direct effect on the

signal quality. When the MDP was positioned >1 cm from the animal, significant fluctuation in the signal was observed and could be explained by the distance of the MDP to the anemone in connection to the weak mixing of the seawater via an air stone, which hampers an even build - up of H_2O_2 in the seawater surrounding the sea anemone. Additionally, bubbles could get trapped on the MDP membrane affecting H_2O_2 diffusion through the membrane. When positioning the MDP in closer contact with the anemone tissue (within the more stagnant water, i.e., the diffusive boundary layer surrounding the animal) more stable measuring signals were observed with a quasi-linear increase in signal over time once the MDP was poditioned. The combined MDP-FIA system thus enables spatially resolved measurements of H_2O_2 in open or closed systems containing living organisms, and this opens for a wide range of applications in the biological sciences, where O_2 respirometry is a core technique, which can now be easily combined with quantitative measurements of H_2O_2.

4.5. H_2O_2 Levels in LB medium.

In a third application, the bacterium *Pseudomonas aeruginosa* was grown in diluted LB-broth medium. The autoclaved medium exhibited a high H_2O_2 background level (~17-18 µM in the diluted sample) causing a high baseline signal in the FIA. After addition of the bacteria, a drop in the signal intensity was observed due to catalase activity of the bacteria leading to H_2O_2 consumption. Such signal behavior was observed with direct FIA measurements of H_2O_2 as well as with FIA–MDP based measurements and measurements with an electrochemical H_2O_2 sensor (Figure S2). Such high H_2O_2 background levels were also confirmed by adding catalase to the reaction mixture (MDP-FIA) or to a LB medium blank, which was measured subsequently to finishing the experiment (DI). This illustrates the importance of careful assessment of background H_2O_2 levels in sample media, typically assumed to contain no H_2O_2. The autoclaved LB medium contained almost 20 µM H_2O_2, while non-autoclaved LB medium at room temperature showed a lower background concentration of ~ 4.9 µM H_2O_2 (Figure 4). This shows that the treatment of the sample medium can have an influence on background H_2O_2 concentrations which needs to be evaluated before setting up an experiment. In addition, it indicates that media used e.g. for isolation and cultivation of bacteria may impose some oxidative stress if they contain such high H_2O_2 background levels. This result was rather unexpected and should be analyzed in more detail in the future. With proper calibration and quantification of background levels of H_2O_2 in apparent blank controls, the combined MDP-FIA system is an ideal instrument for such studies.

5. Conclusion

Coupling MDPs to a FIA system bypasses laborious sample cleaning and pre-treatment steps as well as consumption of the sample. It is possible to measure dynamic changes in H_2O_2 directly in complex sample solutions for extended time periods and without special sample treatment. It was possible to determine concentrations down to the sub µM range with good linear calibration curves. The set-up is highly tunable as the measurement range can be modified to enable broad calibration ranges (e.g. 1 – 100 µM) or highly sensitive measurements over a smaller operational range depending on the used MDP, the syringe pump speed, chemiluminescent reagent concentrations, PMT settings or measurement temperature. Variation of the chemiluminescent (AE) reagent concentration allows a tuning of sensitivity and dynamic range of the H_2O_2 measurements that can compensate e.g. for a lower recovery when sampling H_2O_2 via the MDP membrane and/or at increased perfusion velocities of the carrier solution through the MDP. This tunability makes the MDP-FIA method a potent technique for H_2O_2 determination in many different samples and settings.

In this study we calibrated the combined MDP-FIA system within different H_2O_2 concentration ranges (0- 1000 nM, 0-10 µM and 0 – 100 µM). The LODs depend on the measurement medium and the chosen system settings and can thus be optimized for different media and applications. We conducted a broad cross-sensitivity study to elucidate observed media-effects, including sample pH, salinity, transition metals such as Fe(II), Fe(III), Mn(II) and Cu(II), as well as relevant biomolecules such as urea, L-cysteine and glutathione. We tested other peroxides and ROS such as *tert*-butyl peroxide, peroxynitrite, hypochlorous acid and singlet oxygen and found interfering species, which to the best of our knowledge have not yet been described in literature.

We successfully applied the MDP-FIA system to quantify the dynamics of H_2O_2 in solutions subject to enzyme reactions; we monitored H_2O_2 development in the sea anemone *Exaiptasia pallida* under light stress, and quantified high background levels of H_2O_2 in autoclaved growth medium, which was consumed by the addition of bacteria. We also successfully used it to measure H_2O_2 concentrations in agar plates; thus semi-solid media. The combined MDP-FIA based system thus has a broad applicability for extracellular, near-real time H_2O_2 concentration measurements in both natural and defined samples. The method is minimally invasive, adjustable to different media and concentration ranges, and significantly reduces media effects in comparison to direct FIA-based measurements. While we have focused on H_2O_2 measurements in this study, the system can also be used for chemiluminescent reaction-based quantification of other chemical species [69–71] including ROS such as superoxide [72–74], where suitable chemiluminescent detection schemes have been described.

Acknowledgements

We thank Whitney King (Waterville Analytical) for his technical assistance and extensive advice on the use of the FeLume / FIA system. Sofie L. Jakobsen is thanked for technical assistance setting up the flow injection system. Kasper E. Brodersen is thanked for fruitful discussions. This study was supported by a Sapere-Aude Advanced grant from the Danish Research Council for Independent Research | Natural Sciences (MK), a grant by the Danish Research Council for Independent Research | Technical and Production Sciences (MM, KK, MK, PØJ) and an EU Marie Curie Fellowship (VS).

Author Contributions

MM, KK and MK outlined the paper. Experiments were planned and conducted by MM, KK, VS and PØJ. Data analysis was done by MM, KK and VS. MM wrote the method paper with editorial input from VS, KK, PØJ and MK. All authors contributed to the final paper.

Conflict of Interest

The authors declare no conflict of interest. The founding sponsors had no role in the design of the study; in the collection, analyses, or interpretation of data; in the writing of the manuscript, and in the decision to publish the results.

References

1. Nathan, C.; Ding, A. SnapShot: Reactive oxygen intermediates (ROI). *Cell* **2010**, *140*, 8–10, doi:10.1016/j.cell.2010.03.008.

2. Winterbourn, C. C. The Biological Chemistry of Hydrogen Peroxide. In *Methods in Enzymology*; Elsevier Inc., 2013; Vol. 528, pp. 3–25 ISBN 9780124058811.

3. Ebsworth, E. A. V.; Connor, J. A.; Turner, J. J. The Chemistry of Oxygen. In *Comprehensive Inorganic Chemistry*; Bailar, J. C., Emeléus, H. J., Nyhom, R. S., Trotman-Dickenson, A. F., Eds.; Pergamon Press, 1975; p. 794 ISBN 9781483283135.

4. Gligorovski, S.; Strekowski, R.; Barbati, S.; Vione, D. Environmental Implications of Hydroxyl Radicals (•OH). *Chem. Rev.* **2015**, *115*, 13051–13092, doi:10.1021/cr500310b.

5. Gough, D. R.; Cotter, T. G. Hydrogen peroxide: a Jekyll and Hyde signalling molecule. *Cell Death Dis.* **2011**, *2*, 1–8, doi:10.1038/cddis.2011.96.

6. Moßhammer, M.; Kühl, M.; Koren, K. Possibilities and Challenges for Quantitative Optical Sensing of Hydrogen Peroxide. *Chemosensors* **2017**, *5*, 28, doi:10.3390/chemosensors5040028.

7. Downs, C. A.; Fauth, J. E.; Halas, J. C.; Dustan, P.; Bemiss, J.; Woodley, C. M. Oxidative stress and seasonl coral bleaching. *Free Radic. Biol. Med.* **2002**, *33*, 533–543.

8. Cohen, H. J.; Tape, E. H.; Novak, J.; Chovaniec, M. E.; Liegey, P.; Whitin, J. C. The Role of Glutathion Reductase in Maintaining Human Granulocyte Function and Sensitivity to Exogenous H2O2. *Blood* **1987**, *69*, 493–500.

9. Stone, J. R.; Yang, S. Hydrogen Peroxide: A Signaling Messenger. *Antioxid. Redox Signal.* **2006**, *8*, 243–270, doi:10.1089/ars.2007.1957.

10. Goyen, S.; Pernice, M.; Szabó, M.; Warner, M. E.; Ralph, P. J.; Suggett, D. J. A molecular physiology basis for functional diversity of hydrogen peroxide production amongst Symbiodinium spp . (Dinophyceae). *Mar. Biol.* **2017**, *164*, 1–12, doi:10.1007/s00227-017-3073-5.

11. Abrahamsson, K.; Choo, K.; Pedersén, M.; Johansson, G.; Snoeijs, P. Effects of temperature on the production of hydrogen peroxide and volatile halocarbons by brackish-water algae. *Phytochemistry* **2003**, *64*, 725–734, doi:10.1016/S0031-9422(03)00419-9.

12. Collén, J.; Jiménez Del Río, M.; García-Reina, G.; Pedersén, M. Photosynthetic production of hydrogen peroxide by Ulva rigida C. Ag. (Chlorophyta). *Planta* **1995**, *196*, 225–230.

13. Patterson, P. C. O.; Myers, J. Photosynthetic Production of Hydrogen Peroxide by Anacystis nidulans. *Plant*

Physiol. **1973**, *51*, 104–109.

14. Kalavathi, D. F.; Subramanian, G. Hydrogen Peroxide Photoproduction by A Marine Cyanobacterium Oscillatoria boryana BDU 92181 with Potential Use in Bioremediation. *Biosciences Biotechnol. Res. Asia* **2013**, *10*, 929–935.

15. Suggett, D. J.; Warner, M. E.; Smith, D. J.; Davey, P.; Hennige, S.; Baker, N. R. PHOTOSYNTHESIS AND PRODUCTION OF HYDROGEN PEROXIDE BY SYMBIODINIUM (PYRRHOPHYTA) PHYLOTYPES WITH DIFFERENT THERMAL TOLERANCES 1. *J. Phycol.* **2008**, *44*, 948–956, doi:10.1111/j.1529-8817.2008.00537.x.

16. Lesser, M. P. Coral Bleaching: Causes and Mechanisms. In *Coral Reefs: An Ecosystem in Transition*; Dubinsky, Z., Stambler, N., Eds.; Springer Netherlands: Dordrecht, 2011; pp. 405–419 ISBN 978-94-007-0114-4.

17. Tüğsüz, T.; Gök, E.; Ateş, S. Determination of H2O2 Content of Various Water Samples Using a Chemiluminescence Technique. *Turkish J. Chem.* **2003**, *27*, 41–47.

18. Febria, C. M.; Lesack, L. F. W.; Gareis, J. A. L.; Bothwell, M. L. Patterns of hydrogen peroxide among lakes of the Mackenzie Delta, western Canadian Arctic. *Can. J. Fish. Aquat. Sci.* **2006**, *63*, 2107–2118, doi:10.1139/F06-106.

19. King, D. W.; Cooper, W. J.; Rusak, S. A.; Peake, B. M.; Kiddle, J. J.; Sullivan, D. W. O.; Melamed, M. L.; Morgan, C. R.; Theberge, S. M. Flow Injection Analysis of H2O2 in Natural Waters Using Acridinium Ester Chemiluminescence: Method Development and Optimization Using a Kinetic Model. *Anal. Chem.* **2007**, *79*, 4169–4176.

20. Cooper, W. J.; Zika, R.; Petasne, R. G.; Plane, J. M. C. Photochemical Formation of H2O2 in Natural Waters Exposed to Sunlight. *Environ. Sci. Technol.* **1988**, *22*, 1156–1160.

21. Gonçalves, C.; dos Santos, M. A.; Fornaro, A.; Pedrotti, J. J. Hydrogen Peroxide in the Rainwater of Sao Paulo Megacity: Measurements and Controlling Factors. *J. Braz. Chem. Soc.* **2010**, *21*, 331–339.

22. Jacob, P.; Tavares, T. M.; Rocha, V. C.; Klockow, D. Atmospheric H2O2 field measurements in a tropical environment: Bahia, Brazil. *Atmos. Environ.* **1990**, *24A*, 377–382, doi:10.1016/0960-1686(90)90117-6.

23. Zika, R.; Saltzman, E.; Chameides, W. L.; Davis, D. D. H2O2 Levels in Rainwater Collected in South Florida and the Bahama Islands. *J. Geophys. Res.* **1982**, *87*, 5015–5017.

24. Kelly, T. J.; Daum, P. H.; Schwartz, S. E. Measurements of Peroxides in Cloudwater and Rain. *J. Geophys. Res.* **1985**, *90*, 7861–7871.

25. Reimer, H. The Daily Changing Pattern of Hydrogen Peroxide in New Zealand. *Environ. Toxicol. Chem.* **1996**, *15*, 652–662.

26. Meslé, M. M.; Beam, J. P.; Jay, Z. J.; Bodle, B.; Bogenschutz, E.; Inskeep, W. P. Hydrogen Peroxide Cycling in High-Temperature Acidic Geothermal Springs and Potential Implications for Oxidative Stress Response. *Front. Mar. Sci.* **2017**, *4*, 1–12, doi:10.3389/fmars.2017.00130.

27. Rusak, S. A.; Richard, L. E.; Peake, B. M.; Cooper, W. J. Steady state hydrogen peroxide concentrations across the Subtropical Convergence east of New Zealand. **2005**, 3–4.

28. Yuan, J.; Shiller, A. M. Distribution of hydrogen peroxide in the northwest Pacific Ocean. *Geochemistry Geophys. Geosystems* **2005**, *6*, 1–13, doi:10.1029/2004GC000908.

29. Hopwood, M. J.; Rapp, I.; Schlosser, C.; Achterberg, E. P. Hydrogen peroxide in deep waters from the Mediterranean Sea, South Atlantic and South Pacific Oceans. *Nat. Publ. Gr.* **2017**, 1–10, doi:10.1038/srep43436.

30. Fujiwara, K.; Ushiroda, T.; Takeda, K.; Kumamoto, Y.-I.; Tsubota, H. Diurnal and seasonal dirstribution of hydrogen peroxide in seawater of the Seto Inland Sea. *Geochem. J.* **1993**, *27*, 103–115.

31. Neftel, A.; Jacob, P.; Klockow, D. Long-term record of H2O2 in polar ice cores. **1986**, 262–270.

32. Sigg, A.; Neftel, A. Seasonal variations in hydrogen peroxide in polar ice cores. *Ann. Glaciol.* **1988**, *10*, 157–162.

33. Ho, L. P.; Faccenda, J.; Innes, J. A.; Greening, A. P. Expired hydrogen peroxide in breath condensate of cystic fibrosis patients. *Eur. Respir. J.* **1999**, *13*, 103–106.

34. Sznajder, I. J.; Fraiman, A.; Hall, J. B.; Sanders, W.; Schmidt, G.; Crawford, G.; Nahum, A.; Factor, P.; Wood, L. D. H. Increased Hydrogen Peroxide in the Expired Breath of Patients with Acute Hypoxemic Respiratory Failure. *Clin. Investig. Crit. care* **1969**, *96*, 606–612.

35. Loukides, S.; Horvath, I.; Wodehouse, T.; Cole, P. J.; Barnes, P. J. Elevated Levels of Expired Breath Hydrogen Peroxide in Bronchiectasis. *Am. J. Respir. Crit. Care Med.* **1998**, *158*, 991–994.

36. Long, L. H.; Evans, P. J.; Halliwell, B. Hydrogen Peroxide in Human Urine : Implications for Antioxidant Defense and Redox Regulation. *Biochem. Biophys. Res. Commun.* **1999**, *262*, 605–609.

37. Banerjee, D.; Madhusoodanan, U. K.; Nayak, S.; Jacob, J. Urinary hydrogen peroxide: a probable marker of oxidative stress in malignancy. *Clin. Chim. Acta* **2003**, *334*, 205–209, doi:10.1016/S0009-8981(03)00236-5.

38. Frei, B.; Yamamoto, Y.; Niclas, D.; Ames, B. N. Evaluation of an lsoluminol Chemiluminescence Assay for the Detection of Hydroperoxides in Human Blood Plasma. *Anal. Biochem.* **1988**, *175*, 120–130.

39. Varma, S. D.; Devamanoharan, P. S. Hydrogen Peroxide in Human Blood. *Free Radic. Res. Commun.* **1990**, *14*, 125–131, doi:10.3109/10715769109094124.

40. Giulivi, C.; Hochstein, P.; Davies, K. J. A. Hydrogen Peroxide Production by Red Blood Cells. *Free Radic. Biol. Med.* **1994**, *16*, 123–129.

41. Spector, A.; Garner, W. H. Hydrogen Peroxide and Human Cataract. *Exp. Eye Res.* **1981**, *33*, 673–681.

42. Veal, E. A.; Day, A. M.; Morgan, B. A. Hydrogen Peroxide Sensing and Signaling. *Mol. Cell* **2007**, *26*, 1–14, doi:10.1016/j.molcel.2007.03.016.

43. Yang, J.; Yang, J.; Liang, S. H.; Xu, Y.; Moore, A.; Ran, C. Imaging hydrogen peroxide in Alzheimer's disease via cascade signal amplification. *Sci. Rep.* **2016**, *6*, 35613, doi:10.1038/srep35613.

44. Barnham, K. J.; Masters, C. L.; Bush, A. L. Neurodegenerative diseases and oxidative stress. *Nat. Rev. Drug Discov.* **2004**, *3*, 205–214, doi:10.1038/nrd1330.

45. Yuan, J.; Shiller, A. M. Determination of Subnanomolar Levels of Hydrogen Peroxide in Seawater by Reagent-Injection Chemiluminescence Detection. *Anal. Chem.* **1999**, *71*, 1975–1980, doi:10.1021/ac981357c.

46. Sullivan, D. W. O.; Hanson, A. K.; Kester, D. R. Stopped flow luminol chemiluminescence determination of Fe(II) and reducible iron in seawater at subnanomolar levels. *Mar. Chem.* **1995**, *49*, 65–77.

47. Price, D.; Mantoura, R. F. C.; Worsfold, P. J. Shipboard determination of hydrogen peroxide in the western Mediterranean sea using flow injection with chemiluminescence detection. *Anal. Chim. Acta* **1998**, *371*, 205–215.

48. Cooper, W. J.; Moegling, J. K.; Kieber, R. J.; Kiddle, J. J. A chemiluminescence method for the analysis of H2O2 in natural waters. *Mar. Chem.* **2000**, *70*, 191–200.

49. Miller, G. W.; Morgan, C. A.; Kieber, D. J.; King, D. W.; Snow, J. A.; Heikes, B. G.; Mopper, K.; Kiddle, J. J. Hydrogen peroxide method intercomparison study in seawater. *Mar. Chem.* **2005**, *97*, 4–13, doi:10.1016/j.marchem.2005.07.001.

50. Morris, J. J.; Johnson, Z. I.; Wilhelm, S. W.; Zinser, E. R. Diel regulation of hydrogen peroxide defenses by open ocean microbial communities. *J. Plankton Res.* **2016**, *38*, 1103–1114, doi:10.1093/plankt/fbw016.

51. Schneider, R. J.; Roe, K. L.; Hansel, C. M.; Voelker, B. M. Species-Level Variability in Extracellular Production Rates of Reactive Oxygen Species by Diatoms. *Front. Chem.* **2016**, *4*, 1–13, doi:10.3389/fchem.2016.00005.

52. Valeur, B. *Molecular Fluorescence: Principles and Applications*; Wiley-VCH, 2001; ISBN 3-527-29919-X.

53. Torto, N.; Mwatseteza, J.; Laurell, T. Microdialysis Sampling - Challenges and New Frontiers. *LC GC Eur.* **2001**, 1–6.

54. de Lange, E. C. M. Recovery and Calibration Techniques: Toward Quantitative Microdialysis. In *Microdialysis in Drug Development*; Müller, M., Ed.; 2013; Vol. 4, pp. 3–12 ISBN 978-1-4614-4814-3.

55. Nandi, P.; Lunte, S. M. Recent trends in microdialysis sampling integrated with conventional and microanalytical systems for monitoring biological events: A review. *Anal. Chim. Acta* **2009**, *651*, 1–14, doi:10.1016/j.aca.2009.07.064.

56. Hassett, D. J.; Ma, J. F.; Elkins, J. G.; McDermott, T. R.; Ochsner, U. a; West, S. E.; Huang, C. T.; Fredericks, J.; Burnett, S.; Stewart, P. S.; McFeters, G.; Passador, L.; Iglewski, B. H. Quorum sensing in Pseudomonas aeruginosa controls expression of catalase and superoxide dismutase genes and mediates biofilm susceptibility to hydrogen peroxide. *Mol. Microbiol.* **1999**, *34*, 1082–1093, doi:DOI 10.1046/j.1365-2958.1999.01672.x.

57. Miller, G. W.; Morgan, C. A.; Kieber, D. J.; King, D. W.; Snow, J. A.; Heikes, B. G.; Mopper, K.; Kiddle, J. J. Hydrogen peroxide method intercomparision study in seawater. *Mar. Chem.* **2005**, *97*, 4–13, doi:10.1016/j.marchem.2005.07.001.

58. King, D. W.; Cooper, W. J.; Rusak, S. A.; Peake, B. M.; Kiddle, J. J.; O'Sullivan, D. W.; Melamed, M. L.; Morgan, C. R.; Theberge, S. M. Flow Injection Analysis of H2O2 in Natural Waters Using Acridinium Ester Chemiluminescence: Method Development and Optimization Using a Kinetic Model. *Anal. Chem.* **2007**, *79*, 4169–4176, doi:10.1021/ac062228w.

59. Holzgrabe, U.; Borst, C.; Büttner, C.; Bitar, Y. Quantitative Analysis in Pharmaceutical Analysis. In *Chiral Separations by Capillary Electrophoresis*; Van Eeckhaut, A., Michotte, Y., Eds.; CRC Press, 2009; p. 543 ISBN 978-1-4200-6933-4.

60. Appendix B ICH Guidelines on Validation of Analytical Procedures. In *A Laboratory Quality Handbook of Best Practice*; Singer, D. C., Ed.; ASQ Quality Press, 2001; p. 404 ISBN 0-87389-491.

61. Koren, K.; Jensen, P. Ø.; Kühl, M. Development of a rechargeable optical hydrogen peroxide sensor – sensor design and biological application. *Analyst* **2016**, *141*, 4332–4339, doi:10.1039/C6AN00864J.

62. Grajales, A.; Rodríguez, E. Morphological revision of the genus Aiptasia and the family Aiptasiidae (Cnidaria, Actiniaria, Metridioidea). *Zootaxa* **2014**, *3826*, 55–100, doi:10.11646/zootaxa.3826.1.2.

63. You, Y.; Nam, W. Designing photoluminescent molecular probes for singlet oxygen, hydroxyl radical, and iron–oxygen species. *Chem. Sci.* **2014**, *5*, 4123–4135, doi:10.1039/C4SC01637H.

64. Bregnhøj, M.; Westberg, M.; Jensen, F.; Ogilby, P. R. Solvent-dependent singlet oxygen lifetimes: temperature effects implicate tunneling and charge-transfer interactions. *Phys. Chem. Chem. Phys.* **2016**, *18*, 22946–22961, doi:10.1039/C6CP01635A.

65. Hasan, H. R.; Jabir, R. J.; June, M.; June, M. Oxidative stress status , Nitric oxide and Peroxynitrite levels in sera and saliva of Iraqi smokers. *J. Pharm. Biol. Chem. Sci.* **2017**, *8*, 1414–1424.

66. Koppenol, W. H.; Moreno, J. J.; Pryor, W. A.; Ischiropoulos, H.; Beckman, J. S. Peroxynitrite, a Cloaked Oxidant Formed by Nitric Oxide and Superoxide. *Chem. Res. Toxicol.* **1992**, *5*, 834–842, doi:10.1021/tx00030a017.

67. Hoegh-Guldberg, O.; Bruno, J. F. The Impact of Climate Change on the World's Marine Ecosystems. *Science (80-.).* **2010**, *328*, 1523–1529, doi:10.1126/science.1189930.

68. Voolstra, C. R. A journey into the wild of the cnidarian model system Aiptasia and its symbionts. *Mol. Ecol.* **2013**, *22*, 4366–4368, doi:10.1111/mec.12464.

69. King, D. W.; Lounsbury, H. A.; Millero, F. J. Rates and Mechanism of Fe(II) Oxidation at Nanomolar Total Iron Concentrations. *Environ. Sci. Technol.* **1995**, *29*, 818–824, doi:10.1021/es00003a033.

70. King, D. W. Role of carbonate speciation on the oxidation rate of Fe(II) in aquatic systems. *Environ. Sci. Technol.* **1998**, *32*, 2997–3003, doi:10.1021/es980206o.

71. Emmenegger, L.; King, D. W.; Sigg, L.; Sulzberger, B. Oxidation kinetics of Fe(II) in a eutrophic swiss lake. *Environ. Sci. Technol.* **1998**, *32*, 2990–2996, doi:10.1021/es980207g.

72. Kustka, A. B.; Shaked, Y.; Milligan, A. J.; King, D. W.; Morel, F. M. M. Extracellular production of superoxide by marine diatoms: Contrasting effects on iron redox chemistry and bioavailability. *Limnol. Oceanogr.* **2005**, *50*, 1172–1180, doi:10.4319/lo.2005.50.4.1172.

73. Rose, A. L.; Moffett, J. W.; Waite, T. D. Determination of superoxide in seawater using 2-methyl-6-(4-methoxyphenyl)- 3,7-dihydroimidazo[1,2-a]pyrazin-3(7H)-one chemiluminescence. *Anal. Chem.* **2008**, *80*, 1215–1227, doi:10.1021/ac7018975.

74. Garg, S.; Rose, A. L.; Godrant, A.; Waite, T. D. Iron uptake by the ichthyotoxic Chattonella marina (Raphidophyceae): Impact of superoxide generation. *J. Phycol.* **2007**, *43*, 978–991, doi:10.1111/j.1529-8817.2007.00394.x.

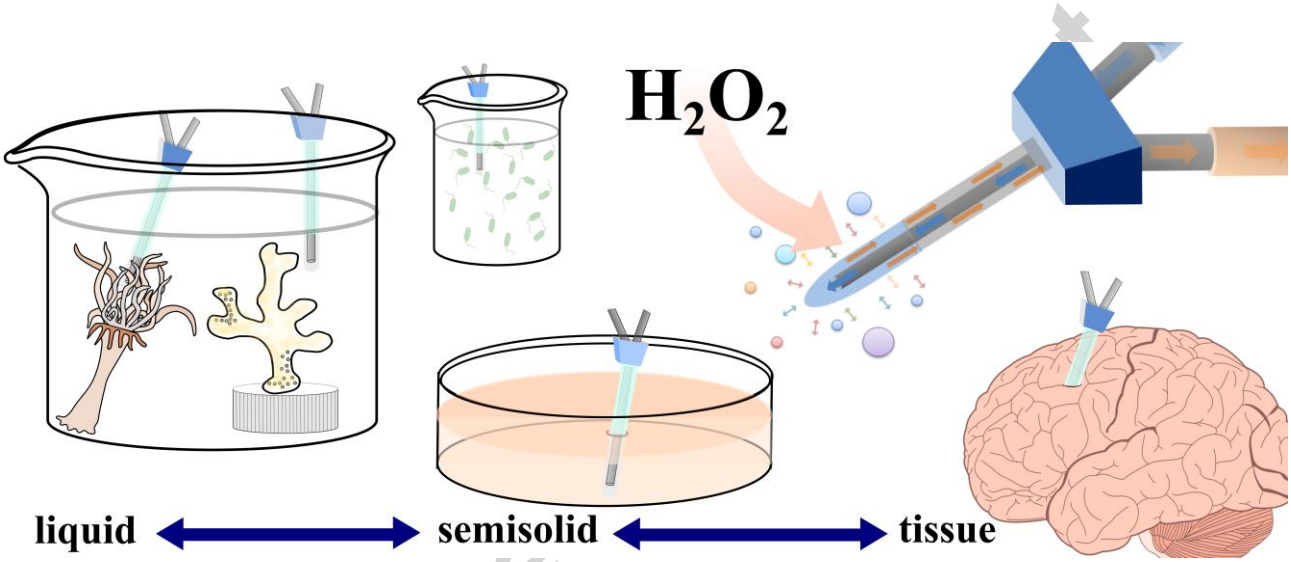

Highlights:

- Successful combination of a FIA system with microdialysis probes for H_2O_2 detection.
- Near real time, chemiluminescence detection of H_2O_2 dynamics in different media.
- Extracellular H_2O_2 dynamics in liquid and semisolid, untreated samples.
- System tunable to different calibration ranges (0–1000 nM; 0–10 µM; 1-100 µM).
- Cross-sensitivity study of potentially interfering species and the chemiluminescent reaction.